MESON PRODUCTION IN DENSE NUCLEAR MATTER*

P. SENGER

for KaoS Collaboration
GSI Darmstadt

Postfach 110541, D-6100 Darmstadt 11, Germany

(Received November 24, 1997)

Pion and Kaon production has been studied in symmetric nucleus–nucleus collisions at beam energies between 0.8 and 1.8 AGeV. The anisotropic azimuthal emission of pions in semi-central collisions can be explained by the emission of high-energy pions in an early stage of the collision and a late "freeze-out" of low-energy pions. In nucleus-nucleus collisions at 1 AGeV, the K^+ multiplicity increases more than linearly both with A (in $A + A$ collisions) and with A_{part} (*i.e.* the number of participating nucleons in Au+Au collisions). This nonlinear behaviour is due to collective effects such as multiple hadron–hadron encounters. According to transport calculations, the large K^+ cross section observed for Au+Au collisions at 1 AGeV is a consequence of a soft nuclear equation of state. The large K^-/K^+ ratio measured in Ni+Ni collisions at equivalent beam energies (compared to $p + p$ collisions) is a signature for an enhanced in-medium K^- production. In order to reproduce the data, transport models have to consider a reduction of the K^- mass in the dense nuclear medium.

PACS numbers: 25.75. Dw

1. Introduction

Collisions between heavy nuclei at bombarding energies of 1–2 AGeV provide the unique possibility to study nuclear matter at high densities. The measured abundances and momenta of emitted particles contain information on the thermal and on the collective energy of the fireball and thus can be linked to the compressibility of nuclear matter. K^+ mesons have a long mean free path in nuclear matter and therefore are well suited to probe the

---

* Presented at the XXV Mazurian Lakes School of Physics, Piaski, Poland, August 27–September 6, 1997.

hot and dense stage of a nucleus-nucleus collision. The K^+ production cross section is predicted to depend on the nuclear equation of state [1–3].

Inside the hot and dense nuclear medium, chiral symmetry is expected to be restored partially with the possible consequence of hadron mass modifications [4–6]. Kaons in particular are regarded as sensitive probes of in-medium effects. According to chiral perturbation theory, the mass of the K^+ mesons weakly increases with increasing nuclear density whereas the mass of the antikaon strongly decreases. The latter effect may lead to K^- condensation in neutron stars and possibly even to the formation of mini black holes in the galaxy [7].

Experiments on kaon and antikaon production in nucleus–nucleus collisions allow to address these fundamental questions. The simultaneous measurement of pions yields supplementary information on the kaon production processes and on the conditions inside the nuclear fireball. This article concentrates on data which recently have been measured with the Kaon Spectrometer [8] at the heavy ion synchrotron (SIS) at GSI in Darmstadt.

2. Pion production in nucleus–nucleus collisions

The experimental study of pion production in nucleus–nucleus collisions allows to gain information on reaction dynamics and on the space-time evolution of the nuclear fireball. A survey of pion production in mass-symmetric heavy-ion collisions at 0.8–1.8 AGeV has been published in [9].

An example for the quality of the pion data as measured by GSI experiments is presented in Fig. 1. It shows the invariant cross sections for the production of charged and neutral pions measured around midrapidity in Au + Au collisions at 1 AGeV by KaoS [10], FOPI [11] and TAPS [12]. All spectra exhibit a low p_t enhancement with respect to a Boltzmann distribution fitted to the high energy part. The $\pi^-/\pi^0/\pi^+$ ratio is in agreement with the isobar model. According to transport models, the pions are produced via the excitation and decay of the Δ_{33} resonance: $NN \rightarrow \Delta N$, $\Delta \rightarrow \pi N$ [13]. The low-p_t enhancement is regarded as a consequence of the decay kinematics of the Δ resonance.
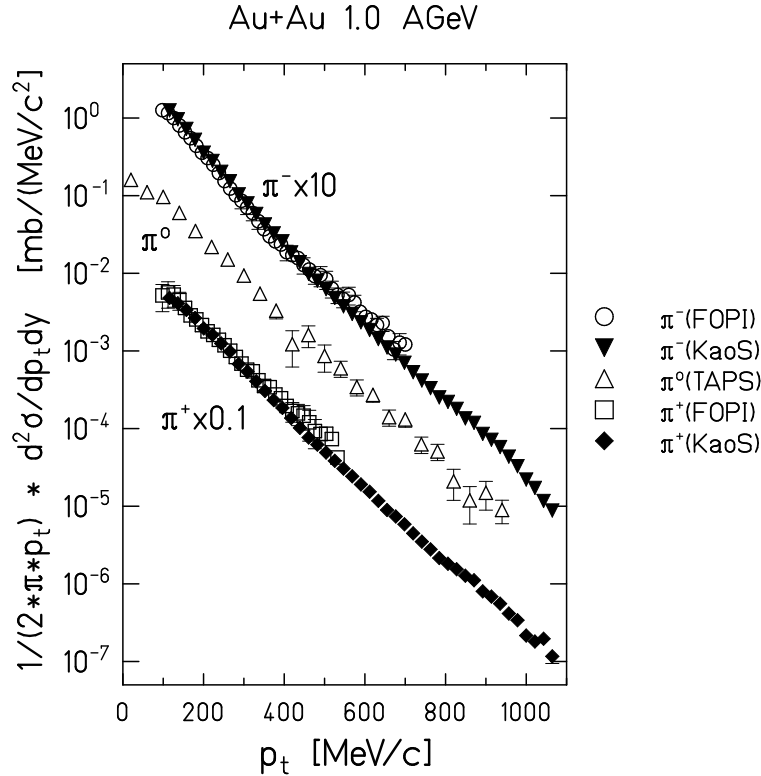
Au+Au 1.0 AGeV

Fig. 1. Invariant pion production cross section measured around midrapidity in Au+Au collisions at 1 AGeV by FOPI (open circles and squares), TAPS (π^o, open triangles) and KaoS (full symbols).

3. The "spectator clock"

The selective trigger of the Kaon spectrometer allows to measure very efficiently high-energy pions which are expected to probe the dense and early stage of the collision [14]. In Au+Au reactions at 1 AGeV it has been found that — in contrast to the low-energy pions- the yield of high-energy pions increases significantly with collision centrality [15]. At this beam energy only 447 MeV are available in a first chance nucleon–nucleon collision. Therefore, the production of pions with a total energy above this value requires collective effects (*i.e.* multiple NN interactions) which are enhanced in central reactions.

In a recent experiment we investigated the pion emission time-scale and its relation to the pion energy. The upper part of Fig. 2 sketches the idea of the "spectator clock" which is based on the observation that pions are
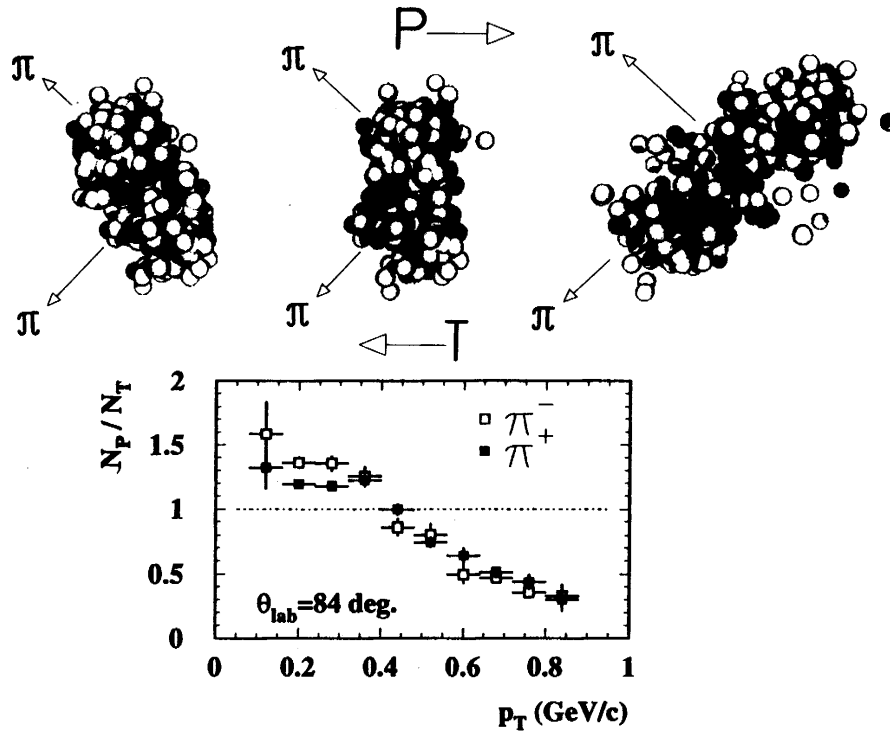
Fig. 2. Upper part: QMD calculation of a semi-central (b=7 fm) Au+Au collision at 1 AGeV [16]. From left to right: picture at 4 fm/c, 8 fm/c and 20 fm/c. The black spheres represent Δ resonances. Pions are measured in the reaction plane at backward angles. Lower part: Ratio of pions emitted to the projectile side (N_P) to the ones emitted to the target side (N_T). The data are taken at $\theta_{\mathrm{lab}} = 84^o$ (0.03< y/y_{beam} <0.10).

shadowed (*i.e.* rescattered and/or absorbed) by the projectile and target spectator remnants in a semi-central nucleus–nucleus collision. Fig. 2 pictures a semi-central ($b = 7$ fm) Au+Au collision at 1 AGeV as calculated by a QMD transport code [16]. The three "snapshots" are taken at 4 fm/c, 8 fm/c and 20 fm/c after the first touch of the nuclei (from left to right). If the pions, for example, are emitted into the reaction plane at backward c.m.-angles (as indicated in Fig. 2) they are shadowed by the projectile spectator in the early phase of the collision and by the target spectator in the late stage.

The lower part of Fig. 2 illustrates the result of the experiment [10]. The data are taken for peripheral and semi-central Au + Au collisions at 1 AGeV. We selected π^+ and π^- mesons which were emitted into the reaction plane ($\Delta\Phi = \pm45°$) at target rapidity ($0.03 < y/y_{\text{proj}} < 0.1$). The figure depicts the ratio N_P/N_T which is the number of pions emitted to the projectile spectator side (N_P) over the number of pions emitted to the target spectator side (N_T). A value of N_P/N_T larger than unity — as found for the low-p_t pions — corresponds to shadowing by the target spectator and hence to a late emission time. For the high-p_t pions, the ratio N_P/N_T is significantly smaller than unity. This observation indicates that these pions are emitted in the early phase of the emission. Coulomb effects do not play a role as π^+ and π^- behave very similarly. The N_P/N_T ratio as shown in the lower part of Fig. 2 corresponds to "antiflow" for low p_t and to "flow" for high p_t pions.

Information on the size of the pion emitting source can be extracted from the π^-/π^+ ratio measured in central Au+Au collisions at 1 AGeV. The total (pion-energy integrated) π^-/π^+ ratio amounts to a value of 1.9 which is in good agreement with the isobar model. We found that the π^-/π^+ ratio decreases (from about 3 at $E_{\text{kin}}^{cm} = 0.05$ GeV) with increasing pion energy and approaches unity above $E_{\text{kin}}^{cm} = 0.4$ GeV. This observation can be explained by a Coulomb shift of the oppositely charged pions. The magnitude of the shift can be extracted from the data. This information allows to deduce the Coulomb potential of the nuclear fireball and — together with the measured number of participating protons — the size of the pion emitting source. The freeze-out radius (which is about 6 fm for high-energy pions) increases with decreasing pion energy [10]. This finding supports the interpretation of the data shown in Fig. 2.

In a first experiment we found that the pions are emitted azimuthaly anisotropic at midrapidity in semi-central Au+Au collisions at 1 AGeV [17]. Recently we have performed a systematic study of this effect in Bi+Bi collisions at incident energies of 0.4, 0.7 and 1.0 AGeV. The anisotropy of the pion azimuthal angular distribution increases with increasing beam energy and with increasing transverse momentum of the pions [18]. In contrast to the nucleons the anisotropy does not vary strongly with the impact parameter [19].

4. Subthreshold kaon production in nucleus–nucleus collisions

The kaon production threshold in free nucleon–nucleon collisions is $E_{\text{beam}} = 1.58$ GeV (for $NN \rightarrow \Lambda K^+N$). Therefore, K^+ production is strongly suppressed in nucleus-nucleus collisions at 1 AGeV. In this case kaon production depends on collective effects which favorably occur in large (and dense) collision systems. Fig. 3 shows the K^+ production cross section

measured for $A + A$ collisions with $A = 12, 20, 58$ and 197 at 1 AGeV. The cross section can be parameterized by $\sigma(K^+) \propto A^{2.0\pm0.2}$. Assuming the reaction cross section $\sigma_R \propto A^{2/3}$, the K^+ multiplicity scales like $M(K^+) = \sigma(K^+)/\sigma_R \propto A^{1.3\pm0.13}$ The K^+ multiplicity increases more than linearly with the number of nucleons. This behaviour is an experimental signature for kaon production via collective effect such as multiple hadron–hadron collisions.

Within the framework of transport models, "subthreshold" kaon production predominantly proceeds via sequential processes involving intermediate pions or Δ resonances: in a first step a Δ (or pion) is produced which collides subsequently with a baryon and produces a kaon [1,20,21]:

(i) $NN \rightarrow N\Delta$ ($\Delta \rightarrow N\pi$) and (ii) $\Delta N \rightarrow KYN$ or $\pi N \rightarrow KY$ with $Y = \Lambda, \Sigma$.

In these processes the pion or Δ serves as an energy reservoir which significantly lowers the K^+ production threshold. Hence the scaling of the K^+ multiplicity with the number of nucleons can be understood quantitatively: (i) the pion multiplicity was found to be proportional to the number of nucleons ($M_\pi \propto A$) and (ii) the probability for a secondary pion–nucleon (or Δ–nucleon) collision scales with the nuclear radius ($\propto A^{1/3}$). Thus the multiplicity of such a sequential process is proportional to $A^{4/3}$.
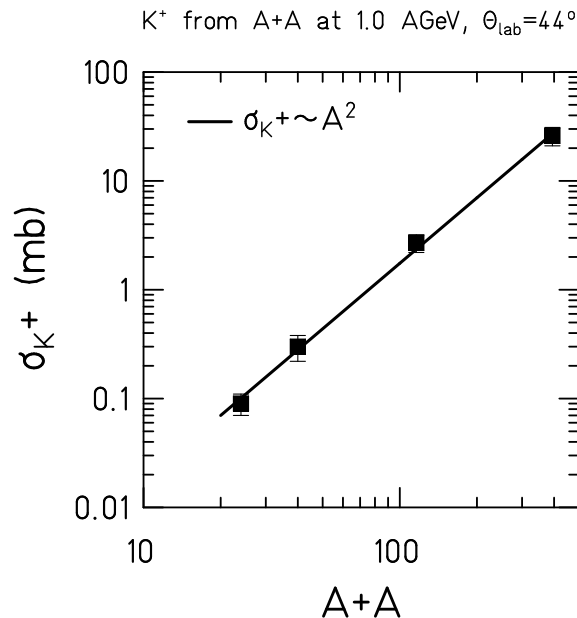

Fig. 3. Total K^+ production cross section from in A+A collisions at 1.0 AGeV as a function of A (preliminary). The data are taken from [22–25].

The simple scaling law $M_{K^+} \propto A^{4/3}$ holds only if the average nuclear density of the reaction volume does not change considerably with the size of the collision system. This is true for impact-parameter integrated $A + A$ collisions where the kaons are produced at nuclear densities of about 2 ρ_o. Fig. 4 shows the K^+ multiplicity as a function of the number of participating nucleons A_{part} in Au+Au collisions at 1 AGeV. The K^+ multiplicity scales according to $M(K^+) \propto A_{\mathrm{part}}^{1.8\pm0.15}$. The K^+ multiplicity scales stronger with A_{part} than with A. This effect might be caused by the increase in nuclear density with increasing centrality (*i.e.* with increasing A_{part}). The pion multiplicity per A_{part} stays constant as a function of A_{part} (open symbols in Fig. 4).
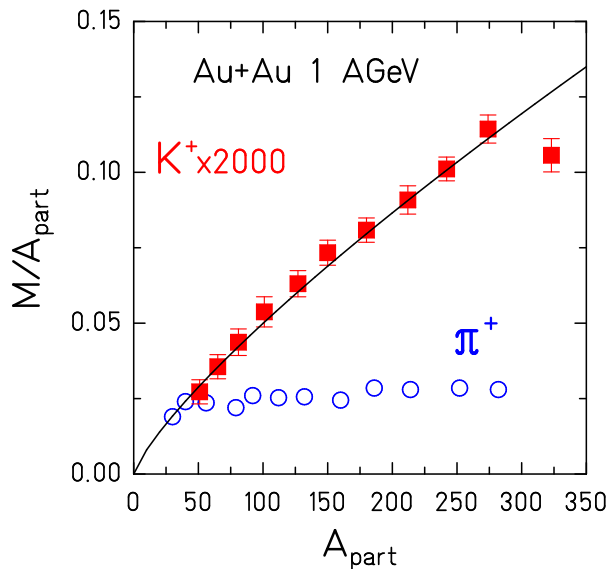

Fig. 4. K^+ and π^+ multiplicity per participating nucleon M/A_{part} as a function of A_{part} measured in Au+Au collisions at 1 AGeV (preliminary [22])

The K^+ mesons have a long mean free path in nuclear matter ($\lambda \approx$ 6 fm) and thus are well suited to probe the dense medium. Nevertheless, the kaons may interact with the nucleons on their out of the collision zone. An observable sensitive to the kaon propagation in nuclear matter is the azimuthal angular distribution. Fig. 5 shows the K^+ azimuthal emission pattern measured around midrapidity in Au + Au collisions at 1 AGeV. The distributions exhibit a pronounced anisotropy for peripheral and semi-central collisions [26]. According to QMD calculations, this azimuthal distribution is due to three effects: *(i)* rescattering at the spectator fragments, *(ii)* Coulomb repulsion and *(iii)* the kaon–nucleon potential in the nuclear medium [27].
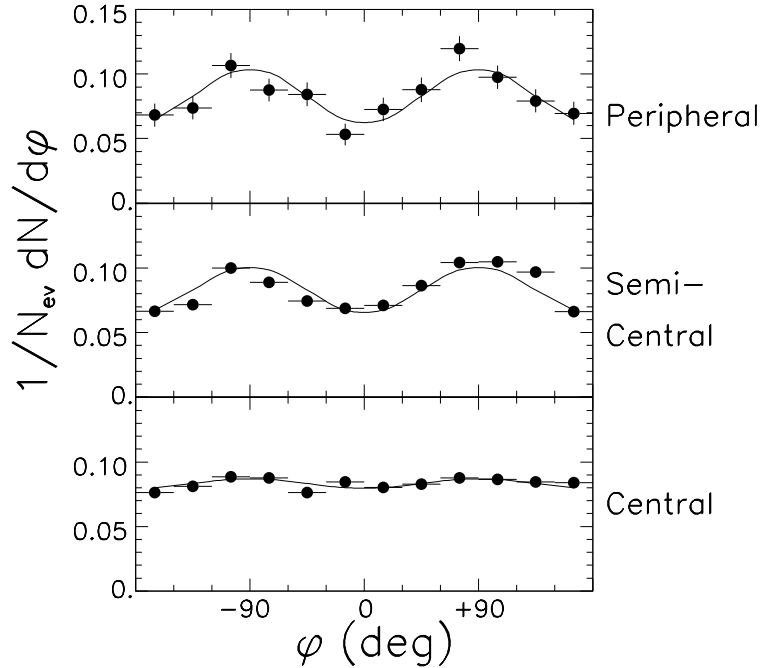
Fig. 5. K^+ azimuthal angular distributions measured in peripheral, semi-central and central Au+Au collisions at 1.0 AGeV. The data are taken within the rapidity interval of $0.4 < y/y_{\mathrm{beam}} < 0.6$ and for transverse momenta $p_t > 0.2$ GeV/c

5. Subthreshold K^+ production and the nuclear equation of state

K^+ production in nucleus-nucleus collisions at subthreshold beam energies is considered as one of the most sensitive probes for the compressibility of nuclear matter [1]. According to transport calculations, the K^+ yield decreases for a "stiff" equation of state. In this case a substantial part of the energy per nucleon is stored in the compression and thus is not available for particle production. Fig. 6 shows the energy per nucleon as a function of nuclear density for a "soft" and a "stiff" equation of state as it is used by a relativistic transport code [28]. The difference in E/A above $\rho = 2\rho_0$ between a soft and a stiff equation of state results in a (factor of 2) difference in the K^+ yield for Au+Au collisions at 1 AGeV. For this system the maximum central density reached in the reaction zone is $\rho = 2.4\rho_0$ and $2.9\rho_0$ for a stiff and a soft equation of state, respectively [28].

Fig. 7 presents the K^+ double differential cross section measured in Au+Au at 1 AGeV in comparison with the result of the RBUU calculation. Evidently the agreement of data and calculation is much better for a soft equation of state [28].
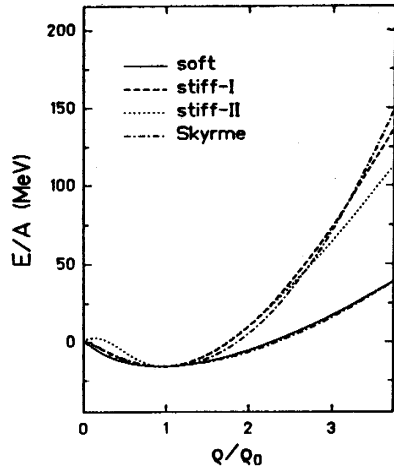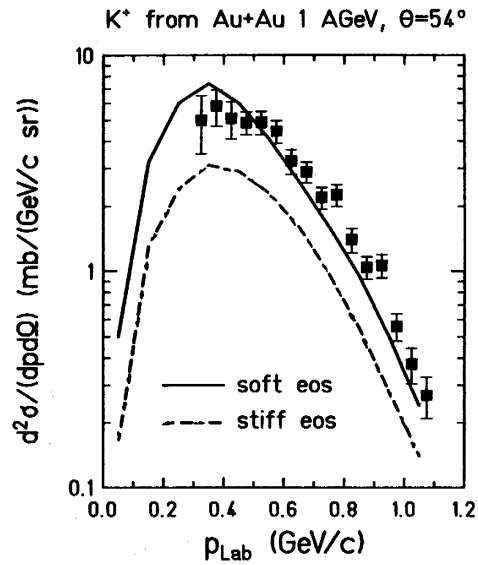
Fig. 6

Fig. 7

Fig. 6. Energy per nucleon as a function of nuclear density ("nuclear equation of state") as calculated in the non-linear $\sigma - \omega$ model and in the Skyrme parameterization. Taken from [28].

Fig. 7. Double differential K^+ cross sections measured in Au+Au collisions at 1 AGeV (full squares, preliminary). The curves are results of a RBUU calculation [28] with a soft equation-of-state (solid line) and a stiff equation-of-state (dashed line).

6. In-medium modifications of the antikaon

The formation of a nuclear fireball in nucleus–nucleus collisions provides the possibility to study the properties of hadrons under extreme conditions. It has turned out, that the produced K-mesons are promising candidates for the experimental study of in-medium modifications.

The properties of kaons and antikaons in dense nuclear matter have been investigated using chiral perturbation theory [4,6], chiral dynamics [5] and a relativistic mean field model [29]. The calculations find an attractive KN (scalar) potential which is related to explicit chiral symmetry breaking due to the large strange quark mass. Due to an additional vector part of the

KN potential, the total KN interaction is weakly repulsive for kaons but strongly attractive for antikaons. Therefore, with increasing nuclear density the K^+ mass is expected to increase weakly whereas the K^- mass should decrease considerably. This effect should lead to a pronounced enhancement of the K^- cross section in nucleus–nucleus collisions at intermediate energies [3,30]. Fig. 8 shows the effective in-medium mass of kaons and antikaons as a function of nuclear density as calculated by various models.
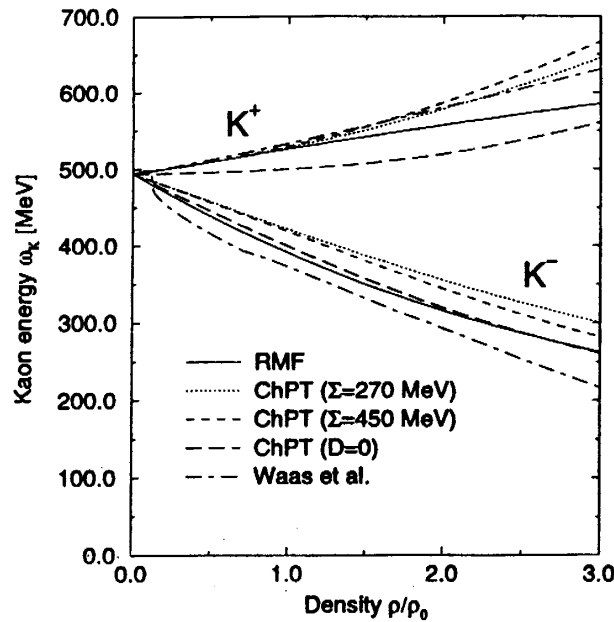

Fig. 8. Effective in-medium mass of kaons and antikaons as a function of nuclear density according to a different calculations. Taken from [29].

The KaoS Collaboration has started to study systematically the in-medium production of K^- and K^+ mesons. In order to find an experimental signature for medium effects on the K^- production cross section, we have compared the K^- yield measured at 1.8 AGeV to the K^+ yield measured at 1.0 AGeV. These two bombarding energies are equivalent with respect to the production thresholds and, therefore, trivial medium effects like Fermi-motion, multiple collisions etc. should approximately cancel in the comparison.

Fig. 9 presents the result of the KaoS experiment [31]. The figure demonstrates that the K^+ yield taken in Ni+Ni collisions at 1 GeV/nucleon agrees roughly with the K^- yield measured at 1.8 GeV/nucleon. This result for nucleus-nucleus collisions is quite different from the K^-/K^+ ratio for proton–proton collisions at equivalent beam energies.
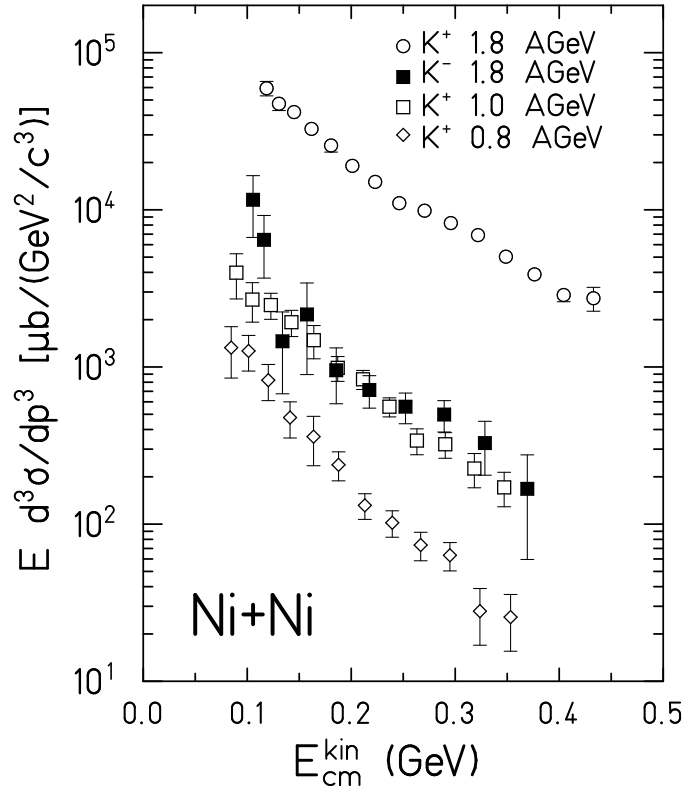
Fig. 9. Invariant kaon production cross sections measured in Ni + Ni collisions at $\Theta_{\text{lab}} = 44^o$ [31].

Fig. 10 shows the available data (including the most recent results from COSY) on inclusive cross sections for K^+ and antikaon production in proton-proton collisions as a function of the energy above threshold [32–35]. The K^+ data exceed the antikaon data by 1–2 orders of magnitude. The lines represent a recent parameterization of the elementary kaon production cross sections [36,37].

Before concluding on an in-medium K^- mass reduction one has to check whether secondary processes like $\pi N \to K^+ Y$ and $\pi N \to K^+ K^- N$ might cause an enhancement of the K^- yield over the K^+ yield in Ni+Ni collisions at equivalent energies. From the measured pion spectra one can estimate that for the beam energy of 1 AGeV the pion yield at$E_{\text{kin}}^{\pi} = 760$ MeV (threshold energy for $\pi N \to K^+ Y$) is about 10 times larger than the pion yield at $E_{\text{kin}}^{\pi} = 1360$ MeV (threshold energy for $\pi N \to K^+ K^- N$) measured at 1.8 AGeV. In addition, near the respective thresholds the cross section $\sigma(\pi^+ p \to K^+ Y)$ exceeds the cross section $\sigma(\pi^- p \to K^+ K^- n)$ by a factor
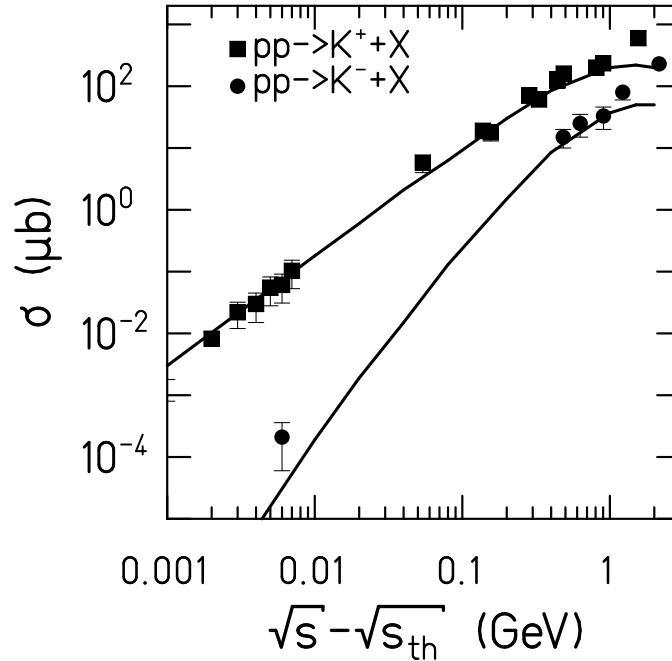
Fig. 10. Kaon and antikaon production cross sections from pp collisions (symbols). The data are taken from [32–35]. Solid lines: parameterization from [36,37].

of 2–3 [38,39]. Therefore, the pion induced kaon and antikaon production cannot explain the K^-/K^+ ratio at equivalent energies. It is very important to simultaneously measure kaons and pions up to very high momenta in order to control the role of pions in kaon production.

The large K^- yield is unexpected since K^- mesons are strongly absorbed in the nuclear medium by strangeness exchange reactions like $K^-N \to \pi\Lambda$. On the other hand, the inverse process might be an additional in-medium source of K^- mesons as pions and hyperons are abundant (the hyperon yield at 1.8 AGeV corresponds roughly to twice the measured K^+ yield). Indeed, recent RBUU calculations claim that (for bare kaon masses, see Fig. 11 left part) the process $\pi Y \to K^-N$ is the most important K^- production channel in Ni+Ni collisions at 1.8 AGeV [21]. This calculations is based on the parameterization of the elementary kaon production cross sections as shown in Fig. 10. Nevertheless, the sum of all K^- production channels considered by the transport calculations is about a factor of 4–5 below the measured data points, if in-medium effects on the K^- mass are omitted (see Fig. 11 left part). In contrast, Fig. 11 (right part) demonstrates that reasonable agreement with the experimental data is achieved by assuming an in-medium reduction of the K^- mass according to $m_K^*(\rho) = m_K^0(1-\alpha \times \rho/\rho_0)$
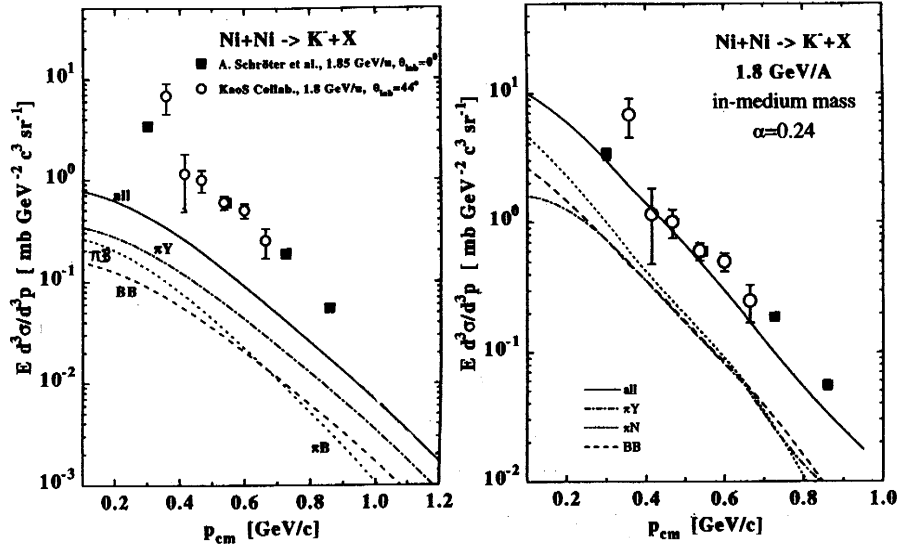
Fig. 11. RBUU calculations of the K^- production cross section in Ni+Ni collisions at 1.8 AGeV [21] compared to the data measured by KaoS at $\Theta_{\text{lab}} = 44°$ (open circles, [31]) and by the FRS at $\Theta_{\text{lab}} = 0°$ (full squares, [40]). Left part: bare K^- mass. Right part: in-medium K^- mass (see text).

with $\alpha = 0.24$. This means, at $\rho = 2\rho_0$ the K^- mass has dropped to half its vacuum value.

The kaon in-medium modification and its effect on the kaon yields from Ni+Ni collisions has been also studied by the Stony Brook group using a RBUU transport code [41]. The result of the calculation is presented in Fig. 12. It shows the K^+/K^- ratio for equivalent beam energies as a function of kaon energy without (dotted line) and with kaon medium effects (solid line). In order to get agreement with the KaoS data (symbols) the authors varied the density dependence of the kaon potentials. Based on the kaon in-medium properties as constrained by the heavy ion data the authors predict K^- condensation in neutron stars and a maximum neutron star mass of about 1.5 solar masses.
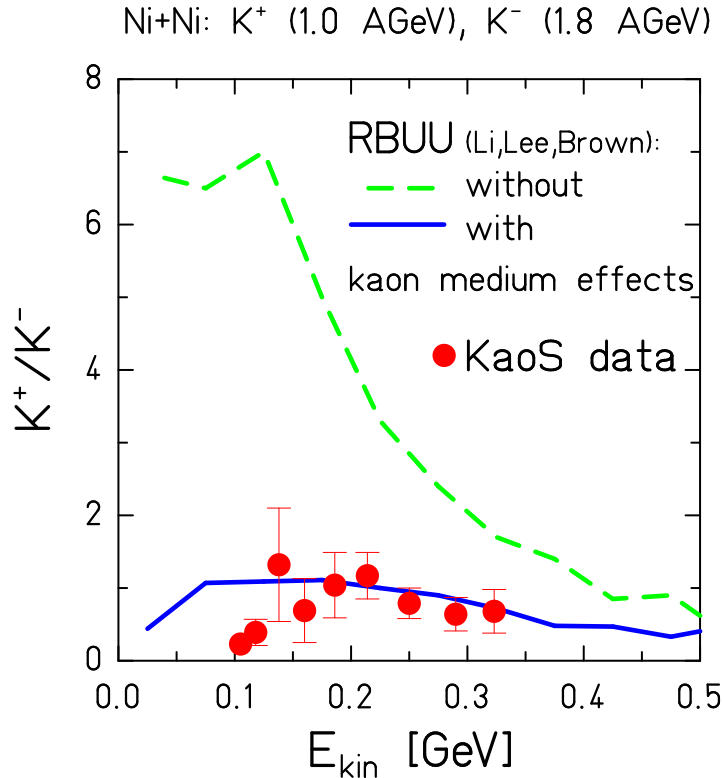
Fig. 12. K^+/K^- ratio for equivalent beam energies as a function of the kaon c.m. kinetic energy (K^+ measured at 1.0 AGeV and K^- at 1.8 AGeV) [41]. Dashed line: without kaon medium effect. Solid line: with kaon medium effect. Full circles: KaoS data [31].

Preliminary data on K^+ and K^- production in C+C collisions at equivalent energies show that the K^- yield at 1.8 AGeV is below the K^+ yield at 1.0 AGeV by about a factor of 3 [24]. This result indicates that the A-dependence for K^- production is stronger than the one for K^+ production although the strong absorption of K^- should weaken the A-dependence.

7. Summary

Recent results on pion and kaon production in nucleus–nucleus collisions at intermediate beam energies have been presented. A collective in-plane motion of pions has been found in non-central Au+Au collisions at 1 AGeV. Low-energy pions are emitted opposite to the spectator matter ("antiflow") whereas the high-energy pions are emitted to the same side ("flow").

This effect is understood as an early emission of high-energy pions and a late "freeze-out" of low-energy pions. In $A + A$ collisions at 1 AGeV, the K^+ multiplicity scales like $M(K^+) \propto A^{1.3\pm0.13}$. In Au+Au collisions, the K^+ multiplicity scales with the number of participating nucleons according to $M(K^+) \propto A_{\mathrm{part}}^{1.8\pm0.15}$. The nonlinear increase is caused by collective effects such as multiple hadron–hadron collisions. The different scaling of $M(K^+)$ with A and A_{part} may be a signature of density effects. Within the framework of transport calculations, the large K^+ cross section observed for Au+Au collisions at 1 AGeV can be reproduced by assuming a soft nuclear equation of state. The large K^-/K^+ ratio measured in Ni+Ni collisions at equivalent beam energies (compared to p+p collisions) is caused by an enhanced production of K^- mesons in the nuclear medium. According to transport models this effect can be explained by a reduction of the K^- mass in dense nuclear matter.

The data presented in this article have been measured and analyzed by the KaoS Collaboration which actually consists of the following persons: P. Koczon, F. Laue, P. Senger, G. Surowka, A. Wagner (GSI), A. Förster, H. Oeschler, C. Sturm. F. Uhlig (TH Darmstadt), E. Schwab, Y. Shin, H. Ströbele (University of Frankfurt), I. Boettcher, B. Kohlmeyer, M. Menzel, F. Pühlhofer (University of Marburg), M. Dębowski, W. Waluś (Jagellonian University Kraków), E. Grosse, L. Naumann, C. Schneider (FZ Rossendorf).

REFERENCES

[1] J. Aichelin, C.M. Ko, *Phys. Rev. Lett.* **55**, 2661 (1985).

[2] T. Maruyama *et al.*, *Nucl. Phys.* **A573**, 653 (1994).

[3] G.Q. Li, C.M. Ko, X.S. Fang, *Phys. Lett.* **B329**, 149 (1994).

[4] D.B. Kaplan, A.E. Nelson, *Phys. Lett.* **B175**, 5 (1986).

[5] S. Klimt *et al.*, *Phys. Lett.* **B249**, 386 (1990).

[6] G.E. Brown *et al.*, *Phys. Rev.* **C 43** , 1881 (1991).

[7] G.E. Brown, H.A. Bethe, *Astron. J.* **423**, 659 (1994).

[8] P. Senger and the KaoS Collaboration, *Nucl. Instrum. Methods Phys. Res.* **A327**, 393 (1993).

[9] C. Müntz and the KaoS Collaboration, *Z. Phys.* **A357**, 399 (1997).

[10] A. Wagner *et al.*, Thesis TH Darmstadt 1996, GSI Scientific Report 1996 .

[11] D. Pelte and the FOPI Collaboration, *Z. Phys.* **A357**, 215 (1997).

[12] O. Schwalb and the TAPS Collaboration, *Phys. Lett.* **B321**, 20 (1994).

[13] S. Huber, J. Aichelin, *Nucl. Phys.* **A573**, 587 (1994).

[14] S.A. Bass *et al.*, *Phys. Rev.* **C50**, 2167 (1994).

[15] C. Müntz and the KaoS Collaboration, *Z. Phys.* **A352**, 175 (1995).

[16] C. Hartnack, private communication.

[17] D. Brill and the KaoS Collaboration, *Phys. Rev. Lett.* **71**, 336 (1993).

[18] D. Brill and the KaoS Collaboration, *Z. Phys.* **A357**, 207 (1997).

[19] D. Brill and the KaoS Collaboration, *Z. Phys.* **A355**, 61 (1996).

[20] C. Fuchs *et al.*, *Phys. Rev.* **C56**, 216 (1997).

[21] W. Cassing *et al.*, *Nucl. Phys.* **A614**, 415 (1997).

[22] M. Mang, Thesis Univ. Frankfurt 1997.

[23] D. Miskowiec and the KaoS Collaboration, *Phys. Rev. Lett.* **72**, 3560 (1994).

[24] W. Ahner and the KaoS Collaboration, *Phys. Lett.* **B393**, 31 (1997).

[25] F. Laue and the KaoS Collaboration, to be published.

[26] Y. Shin and the KaoS Collaboration, submitted for publication.

[27] A. Fässler, private communication.

[28] G.Q. Li, C.M. Ko, *Phys. Lett.* **B349**, 405 (1995).

[29] J. Schaffner *et al.*, NBI-Preprint 96-41.

[30] C.M. Ko, G.Q. Li, *J. Phys.* **G22**, 1673 (1996).

[31] R. Barth and the KaoS Collaboration, *Phys. Rev. Lett.* **78**, 4007 (1997).

[32] CERN H.E.R.A. Report 84-01 (1984).

[33] W.J. Hogan *et al.*, *Phys. Rev.* **166**, 1472 (1968).

[34] J. Balewski *et al.*, *Phys. Lett.* **B388**, 859 (1996).

[35] W. Oelert, W. Eyrich, private communication.

[36] H. Müller *et al.*, *Z. Phys.* **A353**, 103 (1995).

[37] A. Sibirtsev *et al.*, *Z. Phys.* **A358**, 101 (1997).

[38] S.V. Efremov, E.Y. Paryev, *Z. Phys.* **A351**, 447 (1995).

[39] S.V. Efremov, E.Y. Paryev, *Z. Phys.* **A354**, 219 (1996).

[40] A. Schröter *et al.*, *Z. Phys.* **A350**, 101 (1994).

[41] G.Q. Li, C.H. Lee, G.E. Brown, nucl-th/9709024.